Wavelength Dependency of Atmospheric Extinction Coefficient at ETH Zürich HPP Telescope

Nicola Rupf

December 8, 2023

Abstract

This report explores airmass-dependent variations in the atmospheric extinction coefficient, $\kappa(\lambda)$, and color indices in astronomical observations. Theoretical aspects of magnitude and airmass calculation and image data analysis are presented. Experimental findings, particularly for stars with substantial observed airmass ranges, align with literature values and suggest realistic extinction coefficients. However, stars with limited airmass ranges indicate potential systematic discrepancies. Measured color indices B-G (B-V) and B-R largely agree with expectations, though error ranges prevent definitive conclusions. Temperature and humidity fluctuations add further uncertainties, yet the overall comparison supports theoretical expectations. For future observations expanded sample sizes and measurements during diverse conditions are recommended.

1 Introduction

The focus of this study is on investigating the wavelength dependence of the extinction coefficient κ in the context of atmospheric scatterings as well as somewhat equivalently, determining the airmass dependence of the spectral composition of star light better known as a stars color index. The extinction coefficient quantifies the reduction in light intensity as it traverses Earth's atmosphere.
Our starting point is the assumption of a linear dependency on airmass X for the total zero point magnitude m_{ZP}, which combines contributions from the telescope $m_{\text{ZP, instr}}$ and the atmosphere $m_{\text{ZP, atmosphere}}$. The total magnitude m is

$$m = m_{\text{ZP}} + m_{\text{instr}} \tag{1}$$
$$= m_{\text{ZP, atmosphere}} + m_{\text{ZP, instr}} + m_{\text{instr}} \tag{2}$$

Using literature values for m and the formula $m_{\text{instr}}(N,T) = -2.5 \cdot \log_{10}(N/T)$[1] for the instrumental magnitude m_{instr} (which is the magnitude observed by the telescope), where N is the number of counts and T the exposure time, and further assuming that only $m_{\text{ZP, atmosphere}}$ is wavelength dependent and can be written as $m_{\text{ZP, atmosphere}} = \kappa(\lambda) \cdot X$ this yields

$$\kappa(\lambda) \cdot X + m_{\text{ZP, instr}} = m + 2.5 \cdot \log_{10}(N/T) \tag{3}$$

or equivalently

$$\kappa(\lambda) = \frac{m + 2.5 \cdot \log_{10}(N/T) - m_{\text{ZP, instr}}}{X} \tag{4}$$

The unit of count can be chosen to be either photons or ADU (analog to digital units), the telescope's unit of counts. For this telescope the so called A/D Gain is 1.27e^{-1}/ADU, this means that one ADU corresponds to about 0.79 photons[1]. For the entire report we choose ADU as the unit of counts.
Above equations also imply, that if we linearly fit the term $m + 2.5 \cdot \log_{10}(N/T)$ to a magnitude vs. airmass plot, the y-intercept corresponds to $m_{\text{ZP, instr}}$ while the slope is $\kappa(\lambda)$. Note that sometimes $\kappa(\lambda)$ is defined as the extinction coefficient of measured magnitude m_{instr}, while, for the sake of consistency,

we defined it as the extinction coefficient of $m_{\text{ZP, atmosphere}}$. If the total magnitudes m is constant, both definitions are equivalent and, up to a prefactor of -1, even equal (see subsection 4.1).
In astronomical observations, the airmass X parameterizes the path length of light through the atmosphere and is crucial for correcting extinction effects, also for our model. Two widely used models for airmass calculation are the plane-parallel model and the Pickering model. Using the apparent altitude h, the angle between horizon and star, we shortly discuss these two common models for the airmass. The plane-parallel model assumes a flat surface and diverges for h to zero, whereas more accurate models predict values of $X < 40$. It is described by the formula

$$X_{\text{plane-parallel}}(h) = \frac{1}{\sin h} \tag{5}$$

The Pickering model[2] however, assuming a spherical Earth, calculates airmass as

$$X_{\text{Pickering}}(h) = \frac{1}{\sin(h + 244/(165 + 47h^{1.1}))} \tag{6}$$

At low angles Pickering claims a tenfold increase of accuracy to comparable models and the parameters are based on a least square fit[2]. It is important to keep in mind, that none of these models include corrections for altitudes above sea level, where $X < 1$ is possible, and that they do not account for any atmospheric variables. Therefore both models can be seen as guidelines, although the Pickering model certainly is more precise.
Color indices in astronomy, such as the B-V color index, quantify the color of stars by comparing their apparent magnitude in different filters[3]. These color indices correspond to specific wavelength ranges. For example, the blue (B) filter typically corresponds to shorter wavelengths around 440 nm, while the visual (V) filter covers a broader range around 550 nm. The B-V index is then defined as

$$(\mathrm{B} - \mathrm{V}) \coloneqq m_{\mathrm{B}} - m_{\mathrm{V}} \tag{7}$$

where m_{B} and m_{V} are the apparent (measured) magnitudes in the blue and visual filters, respectively. The B-V color index is widely used to estimate a star's temperature, with smaller values indicating hotter stars[4].
Both scattering, which is redirecting, and absorption, which happens when a particle absorbs a photons energy, contribute to the extinction of electromagnetic waves travelling through the atmosphere[5]. Scattering from particles much smaller than a given wavelength, usually visible light, is called Rayleigh scattering. It is proportional to λ^{-4} and dominates wavelength dependency in the visible spectrum. Scattering from larger particles is called aerosol scattering or Mie scattering. It involves particles that are comparable in size to the wavelength of light. The scattering efficiency for these larger particles is less dependent on wavelength, resulting in a more uniform interaction across the visible spectrum[6]. For completions sake, another important phenomenon is ozone or Chappuis absorption. In the range of visble wavelengths however, ozone absorption is of a much smaller scale [7] than other extinction processes and we will not further regard it.

2 Methods

2.1 Experimental methods

On the night of the 26th-27th October 2023, we believe the stars HR 45, HR 875, HR 1034, and HR 8622 to be well suited for observation from the HPP building for several reasons: They are dark enough such that the sensitivity of the telescope is not saturated even for exposure times of several seconds, they are observable by the telescope and not covered by the HPP outline (Figure 1), they cover a lot of angular distance with the horizon, they do not rotate and have constant magnitude, and, since they are standard stars, they are well documented and literature values exist. The hardware used consists of a Planewave CDK20 telescope, a 10 µm GM4000HPS mount and a

SBIG STX-16803 CCD camera[1] and will from now on be referred to as telescope. Apart from the frames taken for data reduction (see subsubsection 2.2.1), a loop taking about 45 min per cycle continuously slews between stars and takes 5 images immediately after each other per star and filter. The filters, similar to this[8] set from Baader, are blue (B) 400 nm to 500 nm, green (G) 490 nm to 580 nm, red (R) 600 nm to 690 nm and light (L) covering the entire visible spectrum. Exposure times (see Table 1) are chosen such that the maximum pixel has 5'000-25'000 ADU for rising stars and 10'000-30'000 ADU for falling stars, ensuring that the sensor is not saturated (saturation maximum at 65 535 ADU[1]), but also such that enough counts are measured throughout the whole observations.

	HR 45	HR 875	HR 1034	HR 8622
B	10	15	8	5
G	7	15	7	4
R	3	10	7	4
L	1	3	2	1

Table 1: Exposure times in s during slewing cycle

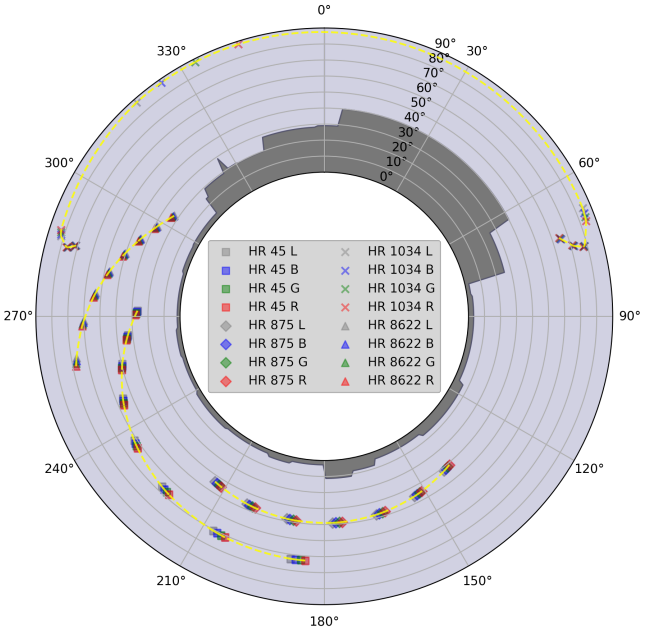

Figure 1: Positions of stars throughout the night. The outline of the the horizon (including the HPP building) is in dark gray.

2.2 Data reduction and analysis

All data reduction and analysis is performed in the web based computational environment Jupiter Notebooks in python. We use the standard packages such as numpy, matplotlib, scipy.optimize and os. More specialized packages include astropy and also photutils. From astropy.visualization we use ZScaleInterval and ImageNormalize to show images and control code. From astropy.io we use fits to access the data stored in the fits files, including the header where information about the image itself (such as time and telescope positioning) is stored. From astropy.stats we use SigmaClip for the background subtraction, see subsubsection 2.2.2. Uses of of photutils are explained appropriately along the way. When referring to pixels we mean single entries in the two dimensional arrays that form the images, given in ADU.

2.2.1 Science images

For each filter we take different types of images. If not stated differently, the operations are to be taken pixel-wise, which in array terms corresponds to along the zero axis.

raw science frame	images of chosen stars, aka. science light
science dark	image of covered sensor, same exposure time as raw science
master dark	median of 15 stacked science darks
flat light	exposure of uniform background
flat dark	image of covered sensor, same exposure time as flat lights
flat dark median	median of 15 stacked flat darks
master flat	subtract flat dark median from each one of 15 flat lights, then take median
$\langle$master flat$\rangle$	average of all pixels in the master flat

For each raw science frame this yields a science image if the following formula[1] is applied

$$\text{science image} = \frac{\text{raw science frame} - \text{master dark}}{\text{master flat}/\langle\text{master flat}\rangle} \tag{8}$$

This, above the fraction bar, subtracts the counts coming from the electronics within the telescope and then divides the result by a factor accounting for uneven exposure due to the peripheral covering of the telescope. The result is a so called science image, a version of the raw science image that is corrected for bias resulting from the telescope.

2.2.2 Background subtraction

Counts resulting from background illumination such as the city's light pollution or the moon also distort magnitude calculations. For each individual image, using Background2D and MedianBackground from the photutils.background package, we subtract a specifically calculated gradient from that image. For the grid size in the Background2D() function we use the size of the corresponding star, in our case between 50x50 and 65x65 pixels. We also import SigmaClip from astropy.stats to identify and discard outliers during the estimation of the background level, helping to improve the accuracy of the background subtraction process. The result is the science image freed from large scale pollution. Note that at this point smaller distortions such as moving airplanes have not been accounted for.

2.2.3 Alignment and stacking

In a next step we combine the 5 images that were taken immediately after for each star position and filter. The astroalign.register() function from the astropy package provides a way to align the 2$^{\text{nd}}$ through 5$^{\text{th}}$ image to the 1$^{\text{st}}$ image by identifying common triangular relations and estimating their affine transformations[9]. Stacking is taking the pixel-wise median and as such combining the 5 aligned images to a single, median image. Instead of also taking the median of the header data, we assume it to vary only very little within the time span of the 5 exposures and assign the header data of the first image to the stacked image.

2.2.4 Count summation

To determine a stars brightness trough a given filter we sum up all of the stars counts, given in ADU, and then convert them to the measured magnitude m_{instr} (see section 1). We assume all observed stars to have a circular shape, even after integrating counts over the entire exposure time and the light passing through the atmosphere. To define which pixel positions actually define the star, we use ApertureStats and CircularAperture from the photutils.aperture package. ApertureStats returns various values including centroid, which is the center of mass or average position of the pixels within a specified aperture, which in turn is defined using CircularAperture and specifying a center and radius.

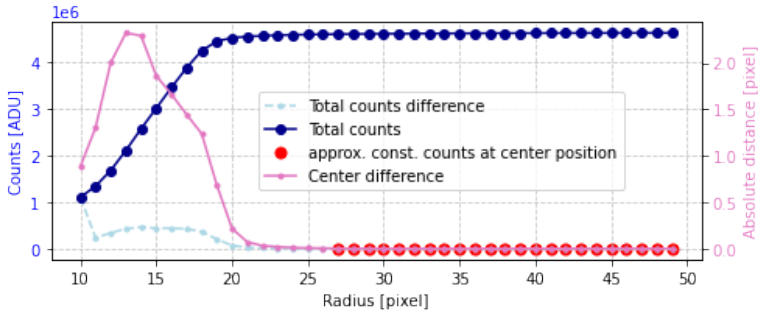

Figure 2: Proof of concept for some image of HR 45 that, given an initial center guess, the center calculation and count summation for an iteration over a range of radii converges. Counts are labelled "approximately constant" if they have not changed more than 0.1 % per step for 5 consecutive steps. Note that this also implies that the center converges and the initial center guess was sufficiently accurate.

After developing a proof of concept (see Figure 2) and seeing that center guesses converge if chosen anywhere in the star, a similar method is applied to determine actual counts. Unlike in the proof of

concept, we determine the center and radius of a given star in a given image separately to improve stability. A loop (see subsubsection A.1.1) iterates up to radii of five times a typical star radius, breaking as soon as the center has not changed more than a tenth of a pixel in absolute value for 10 consecutive iterations. This tolerance is small enough that the function cannot converge outside the star because noise differences are higher and the tolerance is relative in that sense. This was determined through trial and error. The loop breaking also ensures that no neighbouring sources are considered, which sometimes lie only a few star radii apart.
The counts are then determined by iterating over a range of radii, at its maximum certainly containing the star, and creating circular apertures using CircularAperture at each step. Changes in counts are monitored over the last 10 iterations. If the counts stabilize (changing by less than 0.1 %, this tolerance is again determined by trial and error), the function (see subsubsection A.1.2) returns the stable radius and counts. If no stabilization occurs within the specified radii range, it prints a message indicating that the center could not be found. This ensures that the experimenters are aware if either the count or center calculation does not converge.

2.2.5 Airmass

For all images, header values and Pickering model never differ by more than 0.002 airmasses. The differences between header values and the plane-parallel model lie within a range of 0.015 airmasses. We do not know how the telescope's software calculates the values for airmass provided in the header, but in comparison to the models' results it is clear that using even a sophisticated model over the provided values does not significantly improve accuracy. The airmass used for in the experiment is the one provided by the header.

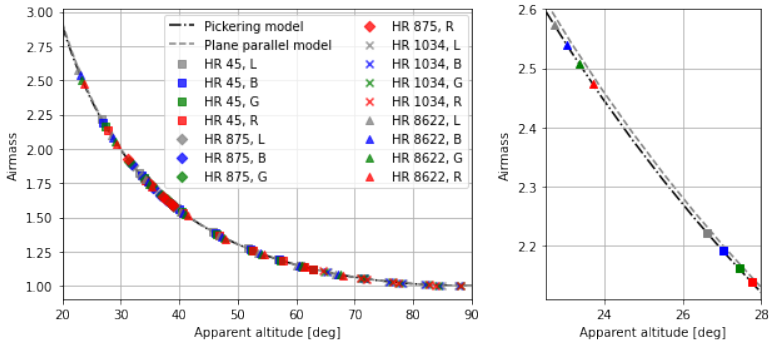

Figure 3: Left: Plot of airmass values provided by the telescope software as well as values from the plane-parallel and Pickering model. Right: Subplot of low apparent altitudes, where the largest differences are to be epecxted.

2.2.6 Error propagation

We only consider errors regarding the counts of the sensor. We assume that for after background subtraction for N counts, the error is of order $\sqrt{N}$. During stacking largest errors stem from moving objects such as airplanes which is why the median provides better results than the mean. Instead of bootstrapping though, we estimate the error of the median to be smaller or equal to the error of the mean, so using mean error propagation is certainly not underestimating the error. The error of the stacked images is then $\propto \frac{\sqrt{N_{\text{science stacked}}}}{\sqrt{5}}$ per pixel. We calculate the error in total counts by summing up the squared error of all pixels contained (or at least the bigger part of the pixel) in the summing radius and taking the square root of this sum. The error in instrumental magnitude is then $\sigma_{\text{instr mag}} \approx -2.5 \cdot \frac{\sigma_{N/T}}{N \ln(10)}$, where $\sigma_{N/T} = \sigma_N / T$ using the exposure time T. The errors for magnitude differences are propagated according to $\sigma_{\text{F}_1 - \text{F}_2} = \sqrt{\sigma_{\text{F}_1}^2 + \sigma_{\text{F}_2}^2}$. We assume that errors of the magnitudes' literature values are negligible, therefore $\sigma_{\text{zero point mag}} = \sigma_{\text{instr mag}}$.
For the error of fitting parameters we simply take the square root of the diagonal elements of the covariance matrix returned by a first order numpy.polyfit(). Uncertainty in fitting the slope and y-incident are not set into relation with measurement uncertainties.

3 Results

3.1 Measured extinction coefficients $\kappa(\lambda)$

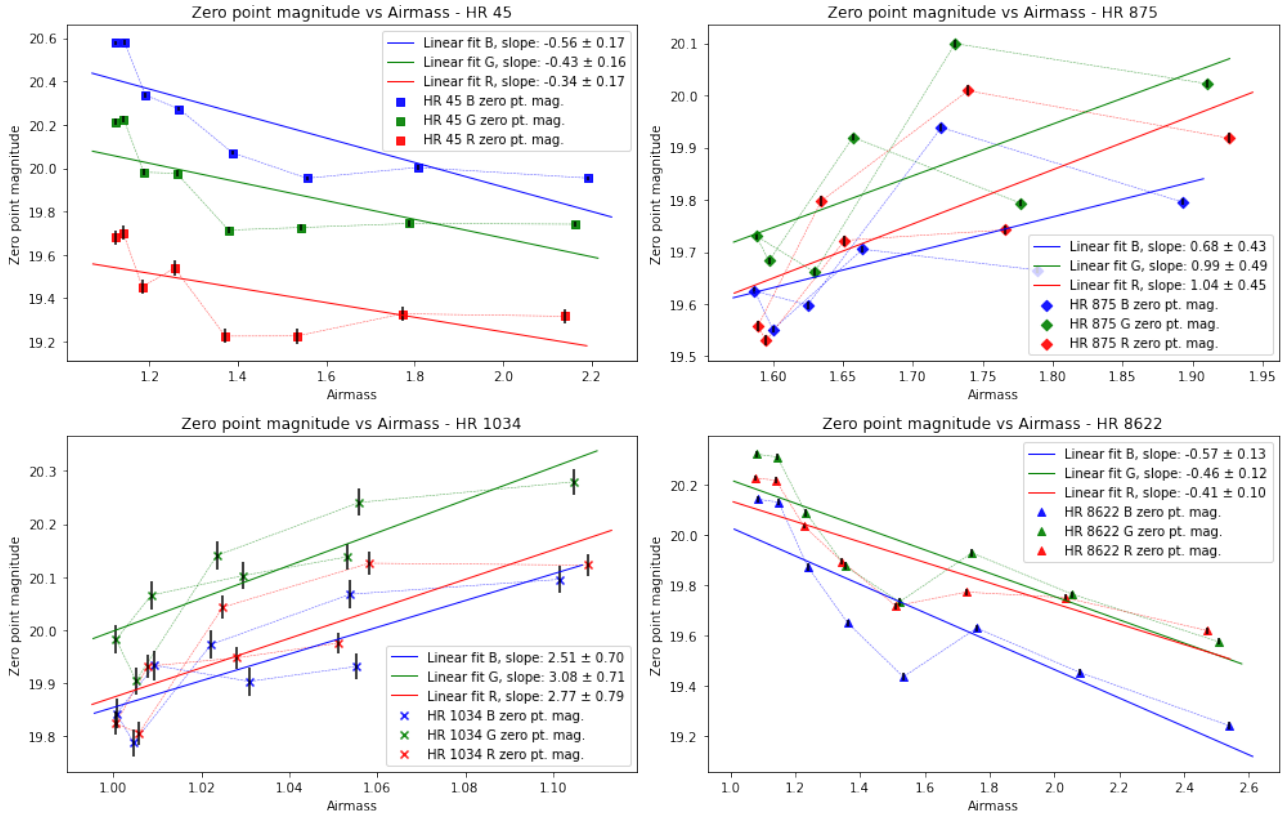

Figure 4: For each star: calculated zero point magnitude for all stars, errors in black. Linear fit for each filter.

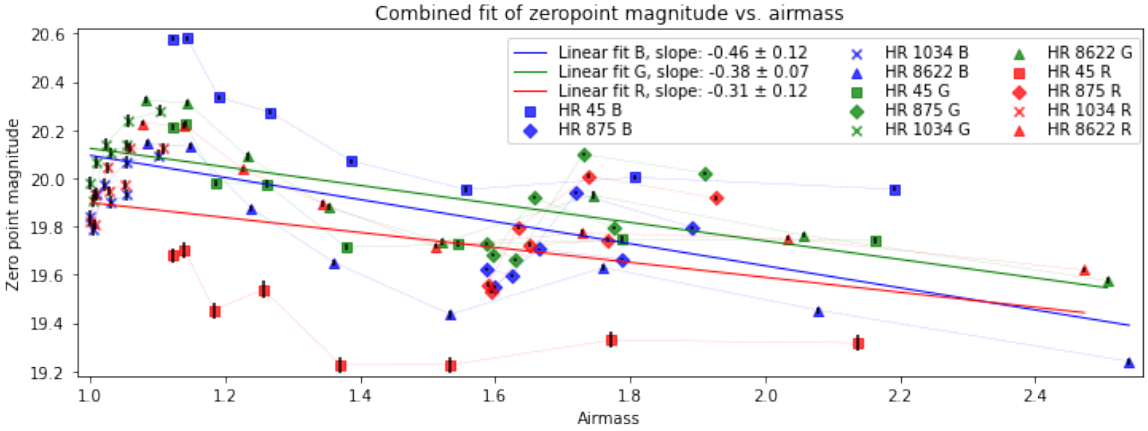

Figure 5: Calculated zero point magnitude for all stars, errors in black. Combined linear fit for each filter.

As elaborated in section 1, using the model $m_{\text{ZP, atmosphere}} = X \cdot \kappa(\lambda)$, the slope of a linear fit to a zero point magnitude plot of a given filter is the extinction coefficient $\kappa(\lambda)$. Following this theory, the y-incident of the linear fit corresponds to $m_{\text{ZP, instr}}$. We get the following experimentally determined values for the extinction coefficient $\kappa(\lambda)$

Filter	$\langle\lambda\rangle$	HR 45	HR 875	HR 1034	HR 8622	Combined
B	450 nm	-0.56 ± 0.17	0.68 ± 0.43	2.51 ± 0.70	-0.57 ± 0.13	-0.46 ± 0.12
G	535 nm	-0.43 ± 0.16	0.99 ± 0.49	3.05 ± 0.71	-0.46 ± 0.12	-0.38 ± 0.07
R	645 nm	-0.34 ± 0.17	1.04 ± 0.45	2.77 ± 0.79	-0.41 ± 0.10	-0.31 ± 0.12

Table 2: Experimentally determined $\kappa(\lambda)$ across all stars and filters, as well as for all stars combined

3.2 Experimental airmass dependence of color indices

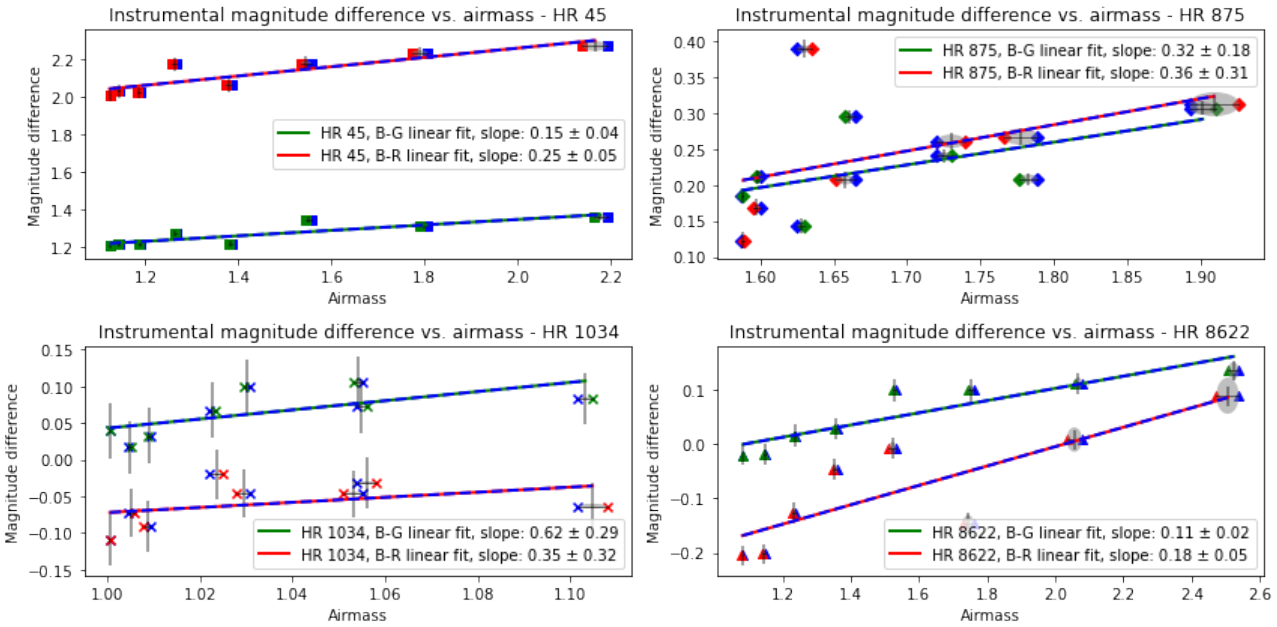

Figure 6: For each star: scatter plot of measured (instrumental) magnitude differences versus airmass and corresponding linear fit to color indices B-G and B-R. Errors in gray.

The used filters are centered at 450 nm, 535 nm and 645 nm for blue, green and red respectively. We consider this mean value as the value of the wavelength for the corresponding filter. This allows for comparison of color indices at different given airmasses, where we identify visual as green. For the different star and filter combinations we get the following color indices (magnitude difference) increases per airmass., where *Combined* considers the data of all stars.

	HR 45	HR 875	HR 1034	HR 8622	Combined
B-G	0.15±0.04	0.32±0.18	0.62±0.29	0.11±0.02	0.17±0.24
B-R	0.25±0.05	0.36±0.31	0.35±0.32	0.18±0.05	0.30±0.44

Table 3: Color indices increases per airmass for B-G and B-R.

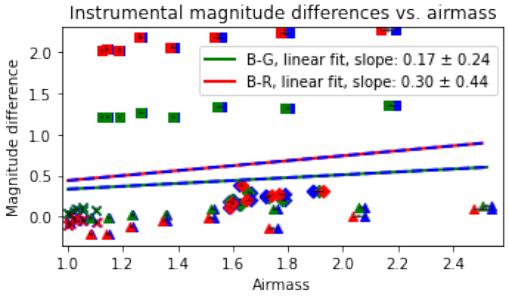

Figure 7: Measured (instrumental) magnitude differences versus airmass and combined linear fit to color indices scatters B-G and B-R. Errors in gray.

Since the images for different filters were taken at different times, they have different airmasses, which reduces comparability. Due to the order of exposure in the loop, this mainly impacts the B-R color index. We chose to assign the mean airmass value of the corresponding magnitude tuple to a given magnitude difference data point. This additional uncertainty is indicated by the gray area in Figure 7 and Figure 6.

4 Discussion

4.1 Comparison of measured extinction coefficient $\kappa(\lambda)$ to literature values

If the observed magnitude $m_{\text{instr}} = -2.5 \cdot \log_{10}(N/T)$ increases with increasing airmass X, corresponding to decreasing counts, it implies that the atmospheric extinction term $\kappa(\lambda) \cdot X$ is somehow contributing to this increase. Since the total magnitude m includes both the telescope and atmospheric contributions and is assumed to be constant for HR 45, HR 875, HR 1034, and HR 8622, an increase in m_{instr} corresponds to a decrease in $m_{\text{ZP}} = m_{\text{ZP, instr}} + m_{\text{ZP, atmosphere}} = m_{\text{ZP, instr}} + \kappa(\lambda) \cdot X$, where we again assume $m_{\text{ZP, instr}}$ to be independent of airmass. Therefore, in a plot of total zero point

magnitude m_{ZP} versus airmass X, we expect $\kappa(\lambda)$ to be negative. Taking Figure 8 as a comparison, we read out literature values of instrumental magnitude extinction coefficients $\kappa_{\mathrm{lit,\ instr}}(450\,\mathrm{nm}) = 0.65 \pm 0.01$, $\kappa_{\mathrm{lit,\ instr}}(535\,\mathrm{nm}) = 0.46 \pm 0.01$, $\kappa_{\mathrm{lit,\ instr}}(645\,\mathrm{nm}) = 0.33 \pm 0.01$ which corresponds to literature values for zero point magnitude extinction coefficients κ_{lit} of $-0.65 \pm 0.01, -0.46 \pm 0.01$ and -0.33 ± 0.01 for blue, green and red respectively. Note that the inaccuracy stems from read-off, inaccuracies of the data itself is not considered. Note also that the values can differ substantially for different conditions. For example, when determining the extinction coefficient for the solar spectrum before noon and after noon, Zenhom et al. measured differences of up to 0.2[10]. However, the comparison of the experimentally determined extinction coefficients $\kappa_{\mathrm{exp}}(\lambda)$ and literature values κ_{lit} across different wavelengths and stars is summarized in the table below.

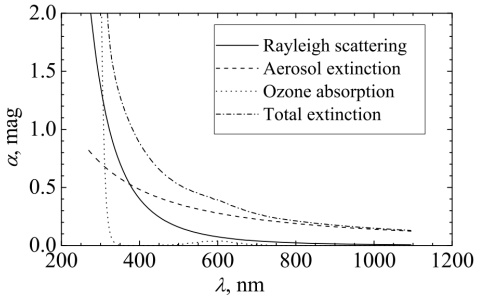

Figure 8: Directly taken from E. Pakštienė and J.-E. Solheim's 2003 paper *Atmospheric extinction corrections for WET observations*[11] (WET = Whole earth telescope). Using a model attributing for Rayleigh scattering, aerosol extinction and ozone absorption they calculate extinction correction coefficients for the Molėtai Observatory (200 m a.s.l.) at airmass $X = 1$.

$\kappa_{\mathrm{exp}}(\lambda) - \kappa_{\mathrm{lit}}(\lambda)$, $[\lambda] = \mathrm{nm}$	HR 45	HR 875	HR 1034	HR 8622	Combined
$\kappa_{\mathrm{exp}}(B) - \kappa_{\mathrm{lit}}(450)$	0.10 ± 0.18	1.14 ± 0.44	2.84 ± 0.71	0.09 ± 0.14	0.19 ± 0.13
$\kappa_{\mathrm{exp}}(G) - \kappa_{\mathrm{lit}}(535)$	0.23 ± 0.17	1.45 ± 0.50	3.51 ± 0.72	0.09 ± 0.13	0.08 ± 0.08
$\kappa_{\mathrm{exp}}(R) - \kappa_{\mathrm{lit}}(645)$	0.32 ± 0.18	1.50 ± 0.46	3.10 ± 0.80	0.08 ± 0.11	0.02 ± 0.13

Table 4: Difference between $\kappa_{\mathrm{exp}}(\lambda)$ and literature values $\kappa_{\mathrm{lit}}(\lambda)$.

It is to be observed, that the experimentally determined values consistently exceeded the literature values, indicating a potential systematic discrepancy. The absence of temperature and humidity considerations, each varying by 10 °C and 40 % respectively, might have contributed to inaccuracies in the data. However, since for wavelength of the literature value we take the mean of the filter spectrum, it is also possible that this assumption is inaccurate and instead a wavelength evaluated from a weighted integral decreased discrepancies. Another interesting observation is that stars that both rise and fall (HR 875 and HR 1034) during the observed time span produce very unexpected data. This might stem from their lower range in airmass, because stars with larger airmass ranges (HR 45 and HR 8622) yield more reliable results. Despite these challenges, the overall comparison is considered satisfactory since the combined result matches the expected and literature well, considering the above mentioned variability. Recommendations for future experiments include expanding the sample size with stars exhibiting larger airmass ranges, employing improved models, and conducting observations on multiple nights to enhance the robustness of the findings.

4.2 Discussion of color indices' dependence on wavelength

To compare the wavelength dependency of measured color indices to literature values we once again make use of the values for the wavelength dependent extinction coefficient calculated by Pakštienė and Solheim[11] and presented in Figure 8. Applying $(\mathrm{B\text{-}G})_{\mathrm{lit}} = \kappa_{\mathrm{lit}}(450\,\mathrm{nm}) - \kappa_{\mathrm{lit}}(535\,\mathrm{nm})$ and analogously for B-R, we obtain literature values for color index increase per airmass of $(\mathrm{B\text{-}G})_{\mathrm{lit}} = 0.19 \pm 0.02$ and $(\mathrm{B\text{-}R})_{\mathrm{lit}} = 0.33 \pm 0.02$, where again we only consider read off uncertainty. A comparison shows

	HR 45	HR 875	HR 1034	HR 8622	Combined
$(\mathrm{B\text{-}G})_{\mathrm{exp}} - (\mathrm{B\text{-}G})_{\mathrm{lit}}$	-0.04 ± 0.05	0.13 ± 0.18	0.43 ± 0.29	-0.08 ± 0.02	-0.02 ± 0.24
$(\mathrm{B\text{-}R})_{\mathrm{exp}} - (\mathrm{B\text{-}R})_{\mathrm{lit}}$	-0.07 ± 0.06	0.04 ± 0.32	0.03 ± 0.34	-0.14 ± 0.06	-0.02 ± 0.45

Table 5: Differences between measured and literature values of color index increases per airmass, B-G and B-R.

Again challenges such as temperature and humidity variations, especially for the stars with smaller airmass ranges, may have contributed to data inaccuracies. However, the overall comparison is considered satisfactory, aligning well with expectations and literature considering the strong dependence on conditions and inherent volatility. Still, error ranges are too large to make conclusive statements.

5 Conclusion

The color indices and extinction coefficients are in agreement with theoretical expectations across large parts of the data set. However, notable discrepancies arise in stars HR 875 and HR 1034, which during our observation covered only 0.1 and 0.3 airmasses, respectively. This may indicate a systematic error, but could also stem from their rising and setting during different atmospheric conditions, whereas HR 45 and HR 8622 covered two or more airmasses and only set during the entire observation period. This is no explanation, but at least puts the inconsistencies into perspective since the combined data of all stars fully agrees with expected and literature, although large error ranges prevent concise statements. Potential factors maybe include measurement inaccuracies or atmospheric effects. In a next step, more stars should be observed during a range of different conditions to provide more robust results.

References

[1] Andreas Bazzon *et al.* Hpp telescope - user manual v3.2, Oct 2023.

[2] Keith A. Pickering. The southern limit of the ancient star catalog. *DIO The International Journal of Scientific History*, vol. 12, Sept. 2002.

[3] Australia Telescope National Facility. The colour of stars. `https://www.atnf.csiro.au/outreach/education/senior/astrophysics/photometry_colour.html`, accessed: 6th Dec. 2023.

[4] Las Cumbres Observatory. Magnitude and color. `https://lco.global/spacebook/distance/magnitude-and-color/`. Explore LCO, Education & Outreach, Science, For Observers.

[5] J. B. Tatum. Absorption, scattering, extinction and the equation of transfer. `https://www.astro.uvic.ca/~tatum/stellatm/atm5.pdf`, 2022. Stellar Atmospheres (last updated: 2022 August 11).

[6] Sean O'Neil. Gpu gems 2, chapter 16. accurate atmospheric scattering. `https://developer.nvidia.com/gpugems/gpugems2/part-ii-shading-lighting-and-shadows/chapter-16-accurate-atmospheric-scattering`, April 2005.

[7] Chris Kreger. Ozone in the atmosphere. `http://www.cotf.edu/ete/modules/ozone/ozatmo.html`, 2005. Last updated: April 28, 2005.

[8] Baader lrgb filter set – cmos-optimized. `https://www.baader-planetarium.com/en/filters/l-rgb-cmos-filters/baader-lrgb-filter-set-%E2%80%93-cmos-optimized.html`, 2008.

[9] Martin Beroiz. Astroalign documentation, revision 56e38920. `https://astroalign.quatrope.org/en/latest/`, 2017.

[10] Heba Zenhom et al. Impact of atmospheric extinction coefficient on the solar spectrum at selective wavelengths at helwan in egypt. *IOP Conference Series: Materials Science and Engineering*, 1269:012011, 2022.

[11] E. Pakštienė and J.-E. Solheim. Atmospheric extinction corrections for wet observations. *Baltic Astronomy*, 12:221–242, 2003. Received December 2, 2002, revised January 13, 2003.

A Appendix

A.1 Code

A.1.1 Center calculation

```
def center_calc(centerguess, data, tolerance=0.01):
    #know from pictures that all stars are certainly within a radius of 40pxl
    radius_range = np.arange(1, 200, 2)

    center_diff_range = []
    consecutive_no_change = 0  # Counter for consecutive iterations with no change

    for r in radius_range:
        aperture = CircularAperture(centerguess, r)
        aperstats = ApertureStats(data, aperture)

        center_diff = np.sqrt( (centerguess[0] - aperstats.xcentroid)**2
                              + (centerguess[1] - aperstats.ycentroid)**2 )
        center_diff_range.append(center_diff)
        centerguess = aperstats.centroid

        if center_diff <= tolerance:
            consecutive_no_change += 1
        else:
            consecutive_no_change = 0  # Reset the counter if there is a change

        if consecutive_no_change >= 10:
            return(np.round(centerguess, decimals=2))

    print(f'fct center_calc could not find center')
```

A.1.2 Count calculation

```
def count_rad(center, data):
    radius_range = np.arange(1, 80, 1)

    count = 0
    last_ten_diff = []

    for r in radius_range:
        aperture = CircularAperture(center, r)
        aperstats = ApertureStats(data, aperture)

        # Check change in the last 10 iterations
        last_ten_diff.append(np.abs(aperstats.sum - count))
        if len(last_ten_diff) > 10:
            last_ten_diff.pop(0)

        #choose tolerance 0.001 because smaller(0.0001) is mainly statistical differences
        if (len(last_ten_diff) == 10
            and
            all(diff <= 0.001 * aperstats.sum for diff in last_ten_diff)):

            return(r, np.round(aperstats.sum, decimals=2))
            break

        count = aperstats.sum
    print(f'fct count_rad could not find center')
```